Implications to Sources of Ultra-high-energy Cosmic Rays from their Arrival Distribution

Hajime Takami [a 1] and Katsuhiko Sato [a,b,c]

[a] *Department of Physics, School of Science, the University of Tokyo, 7-3-1 Hongo, Bunkyo-ku, Tokyo, 113-0033, Japan*

[b] *Research Center for the Early Universe, School of Science, the University of Tokyo, 7-3-1 Hongo, Bunkyo-ku, Tokyo, 113-0033, Japan*

[c] *Institute of Physics and Mathematics for Universe, the University of Tokyo, Kashiwa, Chiba, 277-8582, Japan*

Abstract

We estimate the local number density of sources of ultra-high-energy cosmic rays (UHECRs) based on the statistical features of their arrival direction distribution. We calculate the arrival distributions of protons above 10^{19} eV taking into account their propagation process in the Galactic magnetic field and a structured intergalactic magnetic field, and statistically compare those with the observational result of the Pierre Auger Observatory. The anisotropy in the arrival distribution at the highest energies enables us to estimate the number density of UHECR sources as $\sim 10^{-4}$ Mpc^{-3} assuming the persistent activity of UHECR sources. We compare the estimated number density of UHECR sources with the number densities of known astrophysical objects. This estimated number density is consistent with the number density of Fanaroff-Reily I galaxies. We also discuss the reproducability of the observed *isotropy* in the arrival distribution above 10^{19} eV. We find that the estimated source model cannot reproduce the observed isotropy. However, the observed isotropy can be reproduced with the number density of 10^{-2}-10^{-3} Mpc^{-3}. This fact indicates the existence of UHECR sources with a maximum acceleration energy of $\sim 10^{19}$ eV whose number density is an order of magnitude more than that injecting the highest energy cosmic rays.

Key words: ultra-high-energy cosmic rays

[1] E-mail addresses: takami@utap.phys.s.u-tokyo.ac.jp (H.Takami), sato@phys.s.u-tokyo.ac.jp (K.Sato)

1 Introduction

The origin of ultra-high-energy cosmic rays (UHECRs) has been highly unknown in spite of prolonged effort to construct larger UHECR observatories and to detect more events [1]. In cosmic ray spectrum, a sharply spectral steepening at around 10^{20}eV has been predicted theoretically by interactions with photopion production with cosmic microwave background (CMB) photons, known as Greisen-Zatsepin-Kuz'min (GZK) steepening [2,3]. The feature of this steepening observed by the High Resolution Fly's Eye (HiRes) [4,5] and the Pierre Auger Observatory (PAO) [6,7] implies that astrophysical sources are much more dominant than top-down sources (for a review, see Ref. [8]) at the highest energies, though physical reasons for the extension of the energy spectrum beyond the GZK energies reported by the Akeno Giant Air Shower Array (AGASA) have been not understood yet [9,10]. Several objects to accelerate particles up to 10^{20} eV have been suggested, but there has been little observational evidence which is a UHECR source (see Ref. [8,11] and reference therein).

The arrival distribution of UHECRs has information on the distribution of their sources, also including that on intergalactic and the Galactic magnetic field (IGMF and GMF). The AGASA and PAO reported statistically significant anisotropy at small angular scale in the arrival distribution [12,13,14]. The small-scale anisotropy implies point-like sources, and enables us to constrain the number of nearby UHECR sources. The source number density, n_s, is one of important parameters to investigate the nature of UHECR sources. Comparing the estimated number density with the number densities of known astrophysical objects, we can constrain the object-type of UHECR sources. Several authors have estimated as $n_s \sim 10^{-5}$-10^{-6} Mpc^{-3} using the published AGASA data above 4×10^{19} eV assuming the same injection rate over all sources [15,16,17,18,19], and we also constrained the source number density as 10^{-4} Mpc^{-3}, assuming a model that the injection rate is proportional to the luminosity of galaxies [19].

The PAO reported the correlation between the arrival directions of UHECR above 5.7×10^{19} eV and the positions of nearby active galactic nuclei (AGNs) listed in the 12th Veron-Cetty & Veron catalog [20] within the angular scale of 3.1° [13,14]. However, most of the PAO-correlated AGNs are Seyfert galaxies and LINERs, which have much weaker activity than radio-loud AGNs like Fanaroff-Reily II (FR II) galaxies [21]. To understand whether these galaxies with weak activity are really UHECR sources or not, another information on UHECR sources is required.

The PAO estimated a lower limit of the UHECR source number as 61 based on anisotropy in the arrival distribution of their detected events, simply assuming

Poisson statistics and not taking into account UHECR propagation [14]. This is certainly a lower limit of the number of the sources, but is not quantity which can be compared with astronomical observables because we do not know what radius they are included in. Their number density is an observable. Taking into account UHECR propagation, we can also estimate plausible value of it, not *limit*.

In this study, we simulate the arrival distribution of UHECRs above 10^{19} eV, taking into account their propagation process in intergalactic and the Galactic space. We extract an anisotropy signal from the simulated arrival distribution and then compare this signal with that observed by the PAO above 5.7×10^{19} eV to estimate the source number density. The reports for the correlation by the PAO with nearby large-scale structure [13,14,22,23] show that it plays a crucial role on the arrival distribution of UHECRs. Thus, we adopt the models of the IGMF and source distribution which reproduce the local structure actually observed around the Milky Way, developed in our previous work [18]. We also discuss the isotropy in the arrival distribution at $\sim 10^{19}$ eV and estimate the source number density for the lower energies. The composition is assumed to be pure protons.

This paper is structured as follows. In section 2, our calculation method for calculating UHECR arrival distribution and a statistical method to estimate the source number density are explained. In section 3, the calculation results are shown and we discuss the results and conclude in section 4.

2 Methods

We estimate the number density of UHECR sources as follows. First, we calculate arrival distributions of UHE protons based on our source models with several number densities. Their propagation process in intergalactic and the Galactic space is taken into account. The number of simulated protons and the threshold of their energies are set to the same as those detected by the PAO. Next, auto-correlation functions, which are an indicator of small-scale anisotropy in the arrival distribution, are calculated from our simulated events. Finally, comparing these auto-correlation functions with that calculated from the observed events, we find the best-fit value of the source number density.

We calculate the arrival distribution of UHE protons by a method used in Ref. [19]. A characteristic of this method is to adopt a structured IGMF model which reproduces the observed structure in local universe, developed in Ref. [18]. The strength of the IGMF is normalized at the center of Virgo cluster as $B = 0.0, 0.1, 0.4$ and 1.0μG. This method also enables us to take account of the deflection by GMF. A GMF model with bisymmetric spiral structure proposed

by Ref. [24] and the same model parameters as Ref. [25] is adopted. The maximum distance of UHECR sources is set to 1Gpc, which is comparable with the energy-loss length of Bethe-Heitler pair creation with the CMB. This is sufficient to consider cosmic rays down to 10^{19} eV. There are two improvements for this study. One is the angular resolution of UHECR experiments. In Ref. [19], since we consider the AGASA data, we adopt the angular resolution of $\sim 2^\circ$. In this study, 1° is adopted for the PAO events, which corresponds to the angular resolution of the PAO [14]. The other is to take the non-uniformity of the exposure of ground array into account.

The exposure of ground array is not uniform because of the daily rotation of the earth. Since the variation in right ascension in a day can be neglected [14], the dependence of the exposure is simply written as a function of the declination of arriving cosmic rays, δ, [26],

$$\omega(\delta) \propto \cos(a_0)\cos(\delta)\sin(\alpha_m) + \alpha_m \sin(a_0)\sin(\delta) \tag{1}$$

where α_m is given by

$$\alpha_m = \begin{cases} 0 & \text{if } \xi > 1 \\ \pi & \text{if } \xi < -1 \\ \cos^{-1}(\xi) & \text{otherwise,} \end{cases} \tag{2}$$

and

$$\xi \equiv \frac{\cos(\theta_m) - \sin(a_0)\sin(\delta)}{\cos(a_0)\cos(\delta)}. \tag{3}$$

Here, a_0 is detector's terrestrial latitude, and θ_m is the maximum zenith angle for the experimental cut. For the PAO, $a_0 = 35.2^\circ$ and $\theta = 60^\circ$ are adopted [26].

In this study, we adopt two source models. Both models are constructed from *Infrared Astronomical Satellite Point Source Redshift Survey* (*IRAS* PSCz) catalog of galaxies [27]. The IRAS catalog consists of 14,677 galaxies above 0.6 Jy with redshift and it sky coverage is 84%. So it is the best catalog to reflect the local large-scale structure. We correct the selection effect and galaxies in 16% of unobserved area using the luminosity function estimated by Ref. [28], and then regard subsets of the corrected IRAS galaxies as UHECR source distributions. Each galaxy is adopted as a source with the probability proportional to its luminosity. We perform the source selection 100 times for every n_s. One of the models is a source model with the same cosmic ray injection rate over all sources (called *model A* below), and the other is with the injection

rate proportional to infrared luminosities of galaxies (called *model B* below). The maximum acceleration energy of protons is not dependent on luminosities of the sources. This corrected catalog is also used for the construction of our IGMF model.

Auto-correlation function is one of good indicators of small-scale anisotropy of UHECR arrival distribution. Auto-correlation function is defined as

$$w(\theta) = \frac{1}{2\pi \left|\cos\theta - \cos(\theta + \Delta\theta)\right|} \sum_{\theta \le \phi \le \theta + \Delta\theta} 1[\mathrm{sr}^{-1}], \tag{4}$$

where ϕ is the separation angle of a pair of events. The interval $\Delta\theta$ is set to be 1°. In order to investigate the goodness of fit between the auto-correlation functions calculated from simulated events and observed one, we also define $\chi_{\theta_{\max}}$ as

$$\chi_{\theta_{\max}} = \frac{1}{N_{\mathrm{bin}}} \sqrt{\sum_{n=0}^{N_{\mathrm{bin}}-1} \frac{\left[w(\theta_n) - w_{\mathrm{obs}}(\theta_n)\right]^2}{\sigma(\theta_n)^2}}, \tag{5}$$

where $w(\theta)$ is an average of the auto-correlation function calculated from a source distribution and $\sigma(\theta)$ is the standard deviation of $w(\theta)$ due to the finite number of simulated events. Random event selection is performed 100 times for every source distribution. $w_{\mathrm{obs}}(\theta)$ is the auto-correlation function calculated from observed data. $\theta_{\max}$ is the maximum angular scale to consider the small-scale anisotropy, $N_{\mathrm{bin}} = \theta_{\max}/\Delta\theta$ is the number of angular bins.

3 Results

3.1 Estimation of n_s from the small-scale anisotropy

We estimate UHECR source number density using an anisotropy signal in the 27 events published by the PAO whose energies are above 5.7×10^{19} eV [14]. First, we check the anisotropy signal. Fig. 1 shows auto-correlation function calculated from the 27 events (*histogram*). The auto-correlation function predicted from random distribution weighted by the exposure of the PAO is also shown. The error bars are the standard deviations due to the finite number of events. The event realization is performed 1000 times. We can see statistically significant anisotropy at small angular scale against isotropic distribution. We set $\theta_{\max} = 5°$ in Eq. 5 to extract the small-scale anisotropy. If $\theta_{\max} \sim 10°$ is adopted, main results below are unchanged.

Next, we calculate auto-correlation functions from our simulated arrival distributions of UHE protons, which are compared with the histogram in Fig. 1 to investigate the number density of the sources which can best reproduce the small-scale anisotropy observed by the PAO. If n_s is extremely small, strong anisotropy is expected because only few sources can contribute to the arriving cosmic rays. On the other hand, in the case of much many sources, the arrival distribution is expected to be close to isotropy. Thus, there should be the best-fit value of the number density.

Fig. 2 shows χ_5 calculated for the different number densities of UHECR sources. The normalization of the IGMF strength considered is 0.0 (*crosses*), 0.1 (*triangles*), 0.4 (*squares*), and 1.0 μG (*pentagons*) respectively. The error bars represents the standard deviation of χ_5, which is estimated from 100 realizations of the source distribution. The plots at the same number density are a little shifted horizontally for visibility. Note that UHECR sources within 5 Mpc are artificially neglected in this calculation to reproduce isotropy observed at lower energies ($\sim 10^{19}$ eV). This point will be discussed in section 3.2. Such nearby sources also predict anisotropy stronger than observed on at the highest energies.

In the left figure, χ_5 calculated in the model A is shown. The GMF is considered in the lower panel while not in the upper panel. For $n_s \sim 10^{-7}$ Mpc^{-3}, there is zero or one source within 100 Mpc. This extremely few number of sources leads to anisotropy much stronger than the observational result. Thus, $n_s \sim 10^{-7}$ Mpc^{-3} is too small to reproduce the observed arrival distribution. If, on the other hand, $n_s \sim 10^{-2}$ Mpc^{-3}, which is comparable with the number of bright galaxies, high-precision isotropy of the arrival distribution is realized. This another extreme case cannot also reproduce the observed anisotropy. Thus, χ_5 as a function of n_s has the minimum at the intermediate number density. In the upper panel, χ_5 is minimized at around $n_s \sim 10^{-5}$-10^{-4} Mpc^{-3}, almost independent of the IGMF strength in our IGMF model. In our IGMF model, since about 95% of volume within 100 Mpc has no magnetic field, the highest energy protons are deflected only in the neighbourhood of their sources where the universe is magnetized. If the universe is strongly magnetized, for example, uniformly with $\sim$ 100nG, the source number density is allowed to be smaller because strong deflections makes the arrival distribution to be isotropic even at the highest energies. In the lower panel, χ_5 is minimized at the same number densities. The constrained number density is not dependent on the existence of the GMF since the clustering signal is almost not varied because of the coherence of the GMF. Note that the GMF can changes the arrival directions of UHECRs efficiently and positional correlation with their sources as shown in Ref. [29].

We also estimate the source number density in the model B by similar discussion above. In the right figure, χ_5 in the model B is shown. χ_5 is minimized

at around $n_s \sim 10^{-4}$-10^{-3} Mpc^{-3}, which is about an order of magnitude more than in the model A. In the model B, luminous sources strongly contribute to the arriving cosmic rays and, on the other hand, weaker sources do not almost contribute the flux of cosmic rays though these are counted as sources. Thus, the constrained number density is effectively larger.

The number densities estimated from the anisotropy signal of the PAO based on the two source models (A & B) are consistent with the results of our previous study using the AGASA data [19]. The uncertainty of about one order of magnitude will be reduced by 5 years observation by the PAO, as pointed out in Ref. [19].

The model A and B are two extreme cases. In the model A, all sources are identical. This model can be well applied to astrophysical objects which have hardly personality regarding emitted energy, or strongly active sources like FR II galaxies and Gamma Ray Bursts (GRBs) (though GRBs are transient sources). On the other hand, the model B is applied to objects common in the universe like bright galaxies. When the model B was constructed, the IRAS galaxies with luminosities of 10^7-$10^{12} L_\odot$ were adopted, where $L_\odot$ is the Solar luminosity, 3.826×10^{26} W. The luminosities are over 5 orders of magnitude. The width of magnitude is realized by less active objects like bright galaxies and Seyfert galaxies. In fact, UHECR sources have intermediate nature between the two models. Assumed to be highly active objects, UHECR sources has the number density close to that in the model A. Thus, the number density of UHECR sources can be estimated as $\sim 10^{-4}$ Mpc^{-3}.

Compared with the number densities of several candidates of UHECR sources, this estimated value can constrain the object-type of UHECR sources. Table 1 shows local number densities of several astrophysical objects. The objects which have smaller number density than the estimated one are not main contributors of the arrival highest energy cosmic rays. Both FR II galaxies and BL Lac objects have been plausible UHECR sources theoretically [30,11], but they are not mainly contribute to the flux of UHECRs. Note that this constraint does not reject them as UHECR sources. They are not main contributors. The number density of bright galaxies (defined as $-22 < M_{B_T} < -18$, where M_{B_T} is absolute magnitude in B-band [31]) is much larger than our constraint. The generation of the highest energy cosmic rays is not common phenomena in the local universe. The number density of Seyfert galaxies is an order of magnitude larger than the constrained value, and therefore it is allowed if $\sim 10\%$ of such Seyfert galaxies has activity to accelerate UHECRs. However, Seyfert galaxies are generally not expected to be UHECR sources. For example, the PAO-correlated AGNs, most of all is Seyfert or LINER, do not show significant jet activity [21]. Therefore, there are no reasons for expecting them to accelerate cosmic rays up to the highest energies at all in the jet paradigm. The number density of FR I galaxies is $\sim 10^{-4}$ Mpc^{-3} [34], consistent with the

constraint. FR I galaxy is one of plausible acceleration site up to the highest energies. Centaurus A (Cen A), the nearest PAO-correlated AGNs, is classified into FR I galaxy. At a hot spot in the jet in this galaxy, an estimation of the maximum acceleration energy of protons is $\sim 10^{20.6}$ eV [11]. If the other FR I galaxies have similar configurations, it is possible that FR I galaxies are main contributors of the highest energy cosmic rays.

3.2 Isotropy at around 10^{19} *eV*

At the previous section, we artificially neglect sources within 5 Mpc from the Galaxy. This is because very nearby sources inevitably produce anisotropy in arrival distribution of UHECRs at around 10^{19}eV. Since all observatories on UHECRs have reported isotropy in that energy range [12,35,36]. it is inconsistent with the observational results. We discuss the isotropy in this subsection.

Fig. 3 shows the arrival distributions of protons above 10^{19} eV simulated from a source distribution in the model A with $n_s \sim 10^{-3}$ Mpc^{-3}, which is about one order of magnitude larger than the number density constrained in the previous section. In the left figure, the sources within 5 Mpc are neglected. The number of events is set to 1672, which corresponds to that detected by the PAO [36]. The IGMF strength is $B = 0.4\mu$G.

In the right figure, strong anisotropies appear at the positions of $(\ell, b) \sim (-50^\circ, 20^\circ)$ and $(100^\circ, -85^\circ)$, which are generated by protons injected from Cen A and NGC 253, a famous starburst galaxy, respectively. These distances are 4.6 Mpc and 4.2 Mpc in the IRAS PSCz catalog, respectively [27]. Note that the distance of Cen A is different among many catalogs. If these nearby objects are really UHECR sources, strong anisotropy is inevitably predicted. The PAO reported that the arrival distribution of UHECRs above 10^{19} eV is consistent with isotropic distribution with 95% confidence level [36]. Thus, the anisotropy signals are inconsistent with the PAO results. Such anisotropy is predicted as long as there are UHECR sources in the nearby universe even if $n_s \sim 10^{-3}$ Mpc^{-3} is adopted. On the other hand, the anisotropies disappears in the left figure. This fact is also true in the model B, as shown in Fig. 4. Thus, these nearby objects are not UHECR sources.

In fact, the observed high-level isotropy cannot be easily reproduced by neglecting sources within 5 Mpc. In order to see this, we compare the auto-correlation function of simulated events above 10^{19} eV with that predicted from isotropic distribution. Table 2 shows the fraction of the number of source distributions which can reproduce the arrival distribution consistent with the isotropy within some errors written in the table. σ means the standard deviation of the auto-correlation function calculated from random distribution,

which is due to the finite number of events. The normalization of the IGMF strength considered is 0.1 and 0.4 μG. In the model A, there are few source distributions with $n_s \sim 10^{-4}$ Mpc^{-3} which can reproduce the isotropy within 2σ. Even for $n_s \sim 10^{-3}$ Mpc^{-3}, it is less than 10 though isotropy is found by eye in Figs. 3 and 4. If the number density is $\sim 10^{-2}$ Mpc^{-3}, the isotropy can be well reproduced.

In addition to the structured IGMF, we take account of a uniform turbulent magnetic field with the strength and coherent length of $B_{\rm tur}$, l_c, respectively. Faraday rotation measurements of distant quasars shows $B{l_c}^{1/2} < (1\ {\rm nG})(1\ {\rm Mpc})^{1/2}$ [37]. According to this constraint, we adopt $B_{\rm tur} = 1$ nG and $l_c = 1$ Mpc. The results are also shown in Table 2. We are able to find that the number of the source distributions which can reproduce the isotropy is increased, compared with that without the turbulent field. However, for the estimated number density, the number is still too small to naturally reproduce the isotropy. When the source number density an order of magnitude larger than the estimated one, the number is dramatically increased to 70-80% within 3σ in the model A. If the number density is $\sim 10^{-2}$ Mpc^{-3}, the isotropy can be well reproduced.

It is much larger than the number density estimated based on the small-scale anisotropy at the highest energies. This fact indicates the existence of sources which contributes to lower energy cosmic rays, whose number density is 10^{-2}-10^{-3} Mpc^{-3}. In other words, there are many sources with the maximum acceleration energy of $\sim 10^{19}$ eV. Note that the uniform IGMF does almost not affects the estimation of the number density at the highest energy.

4 Discussion & Conclusion

In this study, we estimated the number density of UHECR sources based on the statistical features of the arrival distribution of UHECRs observed by the PAO. We simulated the arrival distributions of protons above 10^{19} eV, taking into consideration their propagation process in the Galactic and intergalactic space. The IGMF model adopted was associated with the observed large-scale structure. Comparing the simulated arrival distributions with the data observed by the PAO statistically, we estimated the number density which can best reproduce the observational result. The anisotropy signal above 5.7×10^{19} eV led to $n_s \sim 10^{-4}$ Mpc^{-3} which is consistent with that of FR I galaxies, which are a candidate to accelerate protons up to 10^{20} eV. We also focused on isotropy in the arrival distribution at around 10^{19} eV, and then found $n_s \sim 10^{-2}$-10^{-3} Mpc^{-3}, which is one or two order of magnitude larger than that estimated from the anisotropy.

In this calculation, cosmological evolution of UHECR sources is not considered. Since protons with $\sim 10^{19}$ eV can reach the earth from sources at the distance of 1Gpc ($z \sim 0.25$), which is comparable with the energy-loss length of such protons by Bethe-Heitler pair creation, it might be possible that the cosmological evolution could reproduce the isotropy even if the local number density of UHECR sources is comparable with $\sim 10^{-4}$ Mpc^{-3}. However, a typical evolution factor is $(1+z)^3$, and therefore the number density at $z \sim 0.25$ is only twice more than the local one. Such a small factor could not change the estimated number density by two order of magnitude less. The difference between the two estimated number densities is significant.

The difference can be interpreted as the evidence of the existence of UHECR sources which can accelerate protons up to $\sim 10^{19}$ eV assuming the persistent activity of UHECR sources. $n_s \sim 10^{-2}$-10^{-3} Mpc^{-3} is comparable with the number densities of bright galaxies or Seyfert galaxies. The proton acceleration up to 10^{19} eV might be common in the universe. We could also interpret this difference as transient activity to emit UHECRs. If bursting sources, like GRBs, are assumed, apparent number density, which corresponds to n_s estimated in this study, depends on the threshold of UHECR energies because the dispersion of the time-delay is larger at lower energies [38]. However, quantitative discussion on this possibility exceeds the scope of this study. It is next study of ours.

In order to reproduce isotropy in the arrival distribution of UHECRs above 10^{19} eV, sources within 5 Mpc were artificially neglected. In these sources, Cen A, the nearest radio-loud AGN, is involved. The isotropy at around 10^{19} eV implies that it is not UHECR sources in our persistent source model. However, radio-loud AGNs have been plausible site for particle acceleration up to the highest energy [11], and the two of the highest energy events of the PAO are correlated with the position of Cen A within $\sim 3^\circ$. Whether Cen A is really a UHECR source or not is a key to understand the mechanism to generate the highest energy cosmic rays.

If Cen A is not a UHECR source, we can interpret that the source of cosmic rays arriving in the direction of Centaurus is behind Cen A and more distant, so that the strong anisotropy is not generated. The 2 events towards Cen A are also positionally correlated with NGC 5090 with $\sim 3^\circ$, a radio galaxy with the distance of $\sim$ 40 Mpc. This might be a real source though the activity is weak like the other PAO-correlated AGNs. These events are also towards Centaurus cluster whose distance is about 40 Mpc. An idea to generate UHE particles is cluster accretion shock [39,40,41]. However, this scenario can accelerate protons up to $\sim 10^{19}$ eV.

If Cen A is a UHECR source, we propose several possibilities not to generate the anisotropy. One is UHECR composition. In the case of heavy dom-

inated composition at energies above 10^{19} eV, the trajectories of UHECRs are deflected Z times more than those of protons, and the discussion on the isotropy in this paper is not applied. Several composition measurements imply the existence of some fraction of heavy elements for all large uncertainty on hadronic interaction models in extensive air shower [42,43]. The other is that the UHECR production is transient. For a bursting source, the energy of cosmic rays observed at present is in narrow energy range since the time-delay of cosmic rays depends on their energies [38]. In this brief picture, the 2 events are arrived from Cen A, and the lower energies will come in the future. The detailed discussion on the two possibilities is our near future plan.

The estimated number densities have some uncertainty because of the small number of detected events. The uncertainty to determine the number density at the highest energies can be reduced by increasing observed events [19] and significant anisotropy would be observed in the arrival distribution at $\sim 10^{19}$ eV in the near future [44,22]. The dramatically increase of detected events in the near future will provide us more useful information on UHECR sources.

Acknowledgements:

The work of H.T. is supported by Grants-in-Aid from JSPS Fellows. The work of K.S. is supported by Grants-in-Aid for Scientific Research provided by the Ministry of Education, Science and Culture of Japan through Research Grants S19104006.

References

[1] M. Nagano, A.A. Watson, Rev. Mod. Phys. 72 (2000) 689

[2] K. Greisen, Phys. Rev. Lett. 16 (1966) 748

[3] G.T. Zatsepin, V.A. Kuz'min, JETP Lett. 4 (1966) 78

[4] R.U. Abbasi et al., Phys. Rev. Lett., 92 (2004) 151101

[5] R.U. Abbasi et al., Phys. Rev. Lett., 100 (2008) 101101

[6] T. Yamamoto et al., *preprint* arXiv:0707.2638

[7] J. Abraham et al., *preprint* arXiv:0806.4302

[8] P. Bhattacharjee, G. Sigl, Phys. Rep., 327 (2000) 109

[9] M. Takeda et al., Phys. Rev. Lett. 81 (1998) 1163

[10] M. Takeda et al., Astropart. Phys. 19 (2003) 447

[11] D.F. Torres, L.A. Anchordoqui, Rep. Prog. Phys. 67 (2004) 1663

[12] M. Takeda et al., Astrophys. J. 522 (1999) 225.

[13] J. Abraham et al., Science 318 (2007) 938

[14] J. Abraham et al., Astropart. Phys., 29 (2008) 188

[15] H. Yoshiguchi et al., Astrophys. J. 586 (2003) 1211 (erratum 601 (2004) 592)

[16] P. Blasi, D. de Marco, Astropart. Phys. 20 (2004) 559

[17] M. Kachelriess, D. Semikoz, Astropart. Phys. 23 (2005) 486

[18] H. Takami, H. Yoshiguchi, K. Sato, Astrophys. J. 639 (2006) 803 (erratum 653 (2006) 1584)

[19] H. Takami, K. Sato, Astropart. Phys. 28 (2007) 529

[20] M.-P. Veron-Cetty and P. Veron, Astron. & Astrophys. 455 (2006) 773

[21] I.V. Moskalenko, L., Stawarz, T.A. Porter, C.C.Cheung, arXiv:0805.1260

[22] T. Kashti, E. Waxman, JCAP 05 (2008) 006

[23] H. Takami, T. Nishimichi, K. Yahata, K. Sato, in preparation

[24] Y. Sofue, M. Fujimoto, Astrophys. J. 265 (1983) 722

[25] T. Stanev, Astrophys. J. 479 (1997) 290

[26] P. Sommers, Astropart. Phys. 14 (2001) 271

[27] W. Saunders et al., MNRAS 317 (2000) 55

[28] T.T. Takeuchi, K. Yoshikawa, T.T. Ishii, Astrophys. J. 587 (2003) L89 (erratum 606 (2004) L171)

[29] H. Takami, K. Sato, Astrophys. J. 681 (2008) 1279

[30] J. Rachen, P.L. Biermann, Astron. & Astrophys. 272 (1993) 161

[31] J.S. Ulvestad, L.C. Ho, Astrophys. J. 558 (2001) 561

[32] P.C. Hewett, C.B. Foltz, F.H. Chaffee, Astrophys. J. 406 (1993) L43

[33] L. Woltjer, Active Galactic Nuclei, 1990, ed. R.D.Blandford, H. Netzer, L. Woltjer (Berlin:Springer), 1

[34] P. Padovani, C.M. Urry, Astrophys. J. 356 (1990) 75

[35] R.U. Abbasi et al., Astrophys. J., 610 (2004) L73

[36] S. Mollerach et al., *preprint* arXiv:0706.1749

[37] P.P. Kronberg, Rep. Prog. Phys. 57 (1994) 325

[38] J. Miralda-Escude, E. Waxman, Astrophys. J. 462 (1996) L59

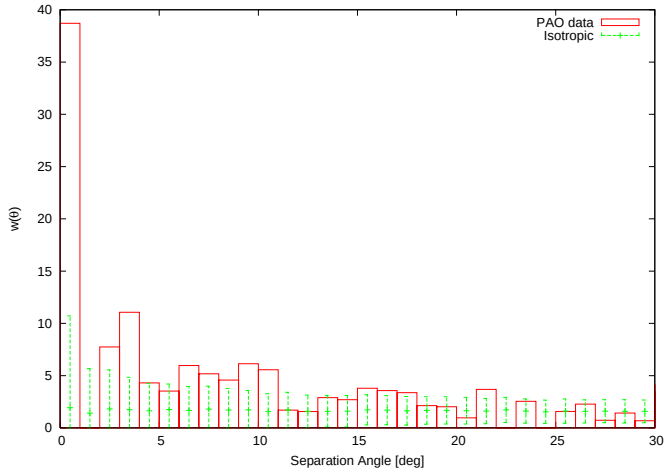

Fig. 1. Auto-correlation functions calculated from the 27 PAO events (*histogram*) and random distribution weighted by the exposure of the PAO. The error bars are the standard deviations due to the finite number of events. The event realization is performed 1000 times.

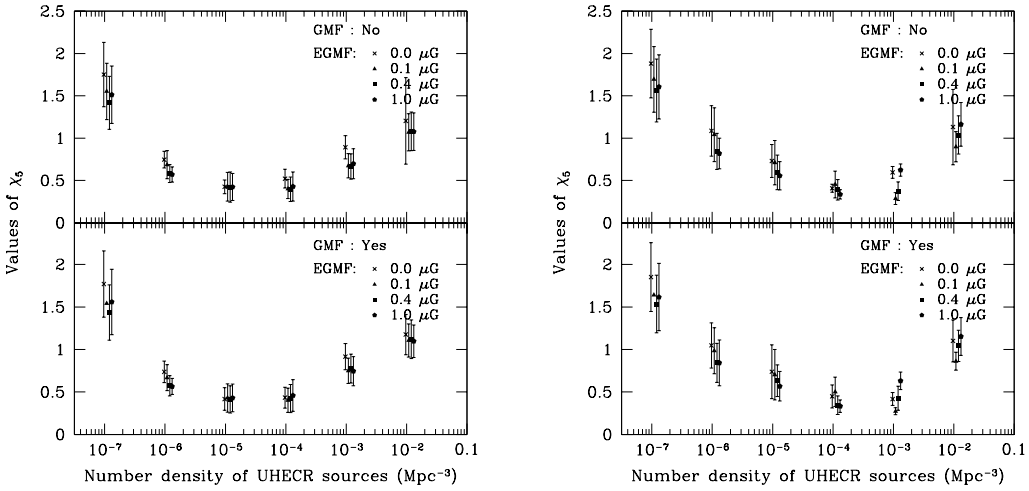

Fig. 2. χ_5 for different number densities of UHECR sources in the model A (*left*) and model B (*right*). The error bars originate from 100 times source selection. The GMF is considered in the lower panel while not in the upper panel.

[39] H. Kang, D. Ryu, T.W. Jones, Astrophys. J., 456 (1996) 422

[40] S. Inoue, F.A. Aharonian, N. Sugiyama, Astrophys. J., 628 (2005) L9

[41] S. Inoue et al., *preprint* astro-ph/0701167

[42] M. Unger et al., *preprint* arXiv:0706.1495

[43] A.V. Glushkov et al., *preprint* arXiv:0710.5508

[44] E. Waxman, K.B. Fisher, T. Piran, Astrophys. J. 483 (1997) 1

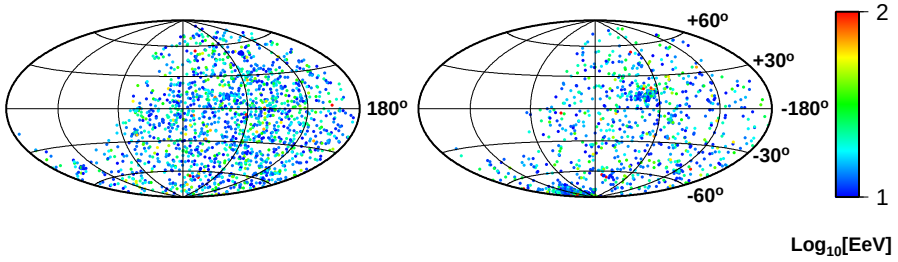

Fig. 3. The arrival distributions of 1672 protons above 10^{19} eV (= 10 EeV) calculated from a source distribution in the model A with $n_s \sim 10^{-3}$ Mpc^{-3} in which the sources within 5 Mpc are included (*right*) and neglected (*left*). The exposure of the PAO is taken into account. The IGMF strength is $B = 0.4\mu$G and the GMF is neglected.

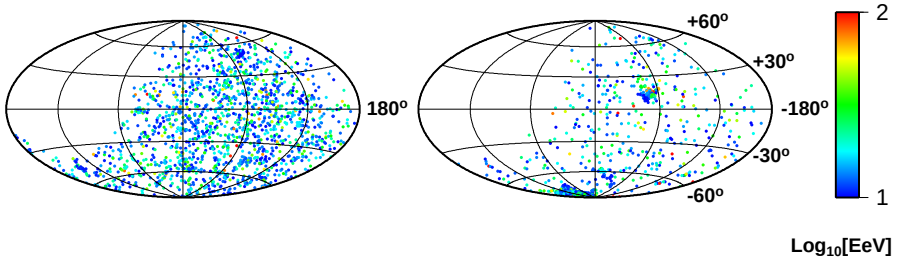

Fig. 4. The same as Fig. 3, but in the model B.

Table 1
Local number densities of several active objects.

Object	Density [Mpc^{-3}]	Reference
Bright galaxy	1.3×10^{-2}	Ref. [31]
Seyfert galaxy	1.25×10^{-3}	Ref. [31]
Bright quasar	1.4×10^{-6}	Ref. [32]
Fanaroff-Reily 1	8×10^{-5}	Ref. [34]
Fanaroff-Reily 2	3×10^{-8}	Ref. [33]
BL Lac objects	3×10^{-7}	Ref. [33]

Table 2
The numbers of the source distributions which satisfy isotropy in the observed arrival distribution of UHECRs above 10^{19} eV within the error bars shown in table, in the case of the model A (without parentheses) and B (in parentheses). The total number of source distributions in each parameter set is 100.

$B_{\rm IGMF}$	0.1 μG				0.4 μG			
$B_{\rm tur}$	0.0 nG		1.0 nG		0.0 nG		1.0 nG	
n_s [Mpc^{-3}]	2σ	3σ	2σ	3σ	2σ	3σ	2σ	3σ
10^{-2}	100(100)	100(100)	100(100)	100(100)	100(100)	100(100)	100(100)	100(100)
10^{-3}	5 (0)	54 (0)	33 (0)	79 (8)	7 (0)	34 (6)	34 (0)	73 (17)
10^{-4}	3 (0)	10 (0)	11 (0)	28 (0)	2 (0)	15 (0)	7 (0)	26 (0)
10^{-5}	0 (0)	2 (0)	0 (0)	9 (0)	0 (0)	0 (0)	0 (0)	6 (0)